

Origin of Network Connectivity and Structural Units in Amorphous SiSe₂

Massimo Celino¹ and Carlo Massobrio²

¹*Ente per le Nuove Tecnologie, l'Energia e l'Ambiente, ENEA, C.R. Casaccia, CP 2400, I-00100 Roma, Italy
and Istituto Nazionale per la Fisica della Materia, Unità di Ricerca, Roma 1, Italy*

²*Institut de Physique et de Chimie des Matériaux de Strasbourg, 23 rue du Loess, BP43 F-67034 Strasbourg Cedex 2, France*
(Received 29 April 2002; published 26 March 2003)

We elucidate the structural properties of amorphous SiSe₂ by first-principles molecular dynamics. The calculated structure factor is in very good agreement with experiments, as well as the number of corner- and edge-sharing tetrahedra. By focusing on the sequences of Si atoms linked via intra- and intertetrahedral bonds, we identify the predominant structural motifs. The sequences involving both corner- and edge-sharing connections are significantly more frequent than those formed exclusively by edge-shared Si atoms. Our results clarify a longstanding controversy on the structure of this prototypical disordered network-forming material.

DOI: 10.1103/PhysRevLett.90.125502

PACS numbers: 61.43.Dq

Fundamental and applied motivations underlie the widespread interest for chalcogenide and oxide AX₂ glasses (A = Ge, Si, X = O, Se, S) [1]. Their atomic structures feature not only short range order as a result of intratetrahedral connections, but also intermediate range order (IRO) involving distances well beyond the first shell of neighbors (typically larger than 5 Å) [2]. The kind of network connectivity which can be attributed to a specific AX₂ disordered system is a highly contentious issue [3]. This debate entails the existence of superstructural motifs (clusters or fragments) in connection to the IRO and the role played by homopolar bonds and miscoordinated atoms in departing from chemical order [4–7]. An additional point of interest is the amount of corner-sharing (CS) and edge-sharing tetrahedra (ES), the two differing by the number of X atoms, one (CS) and two (ES), shared by two AX₄ units. Amorphous SiSe₂ (*a*-SiSe₂) is a very intriguing system in this respect. Its crystalline counterpart consists of parallel chains made of ES tetrahedra only [8]. Intense research efforts, oriented toward the interpretation of Raman and diffraction data, have established that CS tetrahedra are also very much likely to appear in *a*-SiSe₂ [9–12]. In particular, magic angle spinning-nuclear magnetic resonance (MAS-NMR) experiments have given indication for the presence of both CS and ES tetrahedra by introducing the notion of three distinct sites for the Si atoms [13]. Such configurations correspond to Si atoms participating only in CS connections [Si(0)], or in one ES [Si(1)] or two ES [Si(2)] connections, i.e., in zero, one, or two fourfold rings. In this latter case the Si atoms form a chain reminiscent of the crystalline structure. The existence of both corner and edge-sharing tetrahedra has emerged from computer-generated models and classical molecular dynamics (MD) simulations [14,15]. Despite these advances, precise knowledge of the atomic structure of *a*-SiSe₂ has remained elusive. Very recently, Jackson and Grossman have proposed an interpretation of the Raman spectra of *a*-SiSe₂ through a first-principles cluster model

approach, by focusing on isolated molecular entities [16]. These efforts call for the establishment of accurate bulk models of *a*-SiSe₂, providing unambiguous information on the identity and the relative importance of the different constitutive units forming the network.

In this Letter, we study the structure of *a*-SiSe₂ by first-principles molecular dynamics. Our results provide a reliable structural description of the network, as shown by the very good agreement with both neutron diffraction and MAS-NMR data. Amorphous SiSe₂ is to a very large extent chemically ordered with a majority of Si atoms in ES configurations. Focusing on the sequences of three neighboring tetrahedra, Si(1)-Si(2)-Si(1) is predominant among those arranged in chainlike structures with ES connections only. However, we found that the amount of Si(1)- and Si(0)-centered sequences of three tetrahedra is much larger. Their occurrence demonstrates that the most frequent structural subunits in *a*-SiSe₂ involve both ES and CS connections.

In our approach the self-consistent evolution of the electronic structure during the motion is described within density functional theory [17]. We adopted a generalized gradient approximation (GGA) for the exchange and correlation part of the total energy [18]. The valence electrons are treated explicitly whereas norm-conserving pseudopotentials account for the core-valence interactions. Pseudopotentials were generated as in Ref. [19]. The wave functions are expanded in plane waves at the Γ point of the supercell. A cutoff energy of 20 Ry yields accurate and converged properties for the dimer SiSe as well as for crystalline SiSe₂. We considered two systems consisting of stoichiometric compositions of $N = 120$ and $N = 144$ atoms in periodically repeated cubic cells of size 15.61 and 16.56 Å, respectively. The density is equal to the experimental value for *a*-SiSe₂ at $T = 300$ K [10]. For $N = 120$, we positioned randomly the atom in the simulation box, we raised the temperature first to $T = 4000$ K and then gradually lowered it to 1000 K in 15 ps. At $T = 1000$ K the system evolved for additional 9 ps.

The initial configuration for $N = 144$ was obtained by adapting the crystal structure of SiSe_2 to the cubic symmetry. This system is melted and thermalized at $T = 1000$ K for 15 ps. In the two sets of simulations, the distances covered by the atoms in the liquid configurations (more than 25 \AA) ensure that no memory of the initial geometries is maintained. We have generated as much as six amorphous structures by quenching to $T = 300$ K an equivalent number of statistically uncorrelated liquid configurations. Data collection takes place at thermal equilibrium over periods of 3–5 ps for each set of calculations. From this set of partial averages, we extracted the mean values and error bars reported hereafter.

The calculated neutron scattering structure factor shows very good agreement with experiment [10] (Fig. 1). Statistical errors are larger for low k and attain 20% for the FSDP height. We note that, within statistical errors, the position and the height of the peaks and minima are well reproduced over the entire k range. The behavior for low k can be rationalized as follows. Along a given run in the liquid phase, the height of the FSDP changes considerably with time, by varying in between 0.5 and 0.9. Quenching has two main effects on the low k portion of the total structure factor. On the one hand, time fluctuations are strongly reduced. On the other hand, the FSDP height and the first minimum of the structure factor remain very close to the values taken in the parent liquid. As a consequence of this sensitivity to the initial quenching configurations, strong variations among the different partial averages induce large error bars in the mean values of intermediate range properties.

Partial pair correlation functions $g_{\text{SiSi}}(r)$, $g_{\text{SiSe}}(r)$, and $g_{\text{SeSe}}(r)$ are shown in Fig. 2. In $g_{\text{SiSi}}(r)$ the peak at 3 \AA can

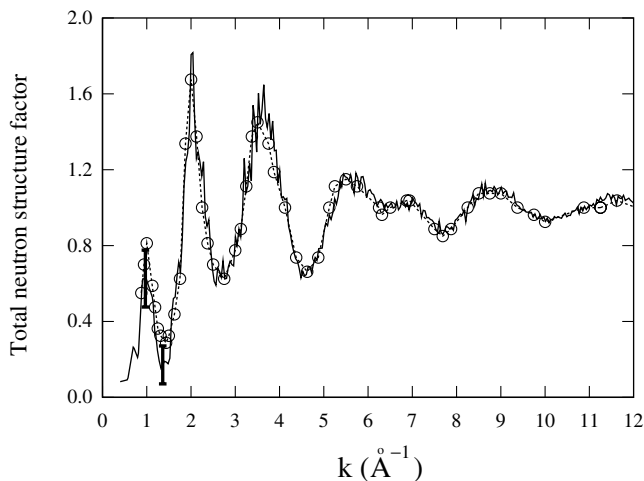


FIG. 1. Calculated total neutron structure factor $S(k)$ of $\alpha\text{-SiSe}_2$ (solid line) at $T = 300$ K. The experimental results (circles connected by dotted lines) are from Ref. [10]. We used scattering lengths of $b_{\text{Si}} = 4.149$ and $b_{\text{Se}} = 7.97$ fm (Ref. [10]). Error bars are given in the low k region at the locations of the FSDP and of the first minimum.

be attributed to ES tetrahedra as proved by the calculation of $g_{\text{SiSi}}(r)$ including only Si atoms in ES configurations. The feature discernible between 2.4 and 2.6 \AA is due to Si—Si homopolar bonds, each Si atom having on average $n_{\text{SiSi}} = 0.06$ nearest neighbors of the same species, i.e., within a given shell of radius 2.6 \AA . We obtain that 1% of the bonds involving Si are homopolar. In the pair correlation function $g_{\text{SeSe}}(r)$ the main peak is due to intratetrahedral second neighbors Se-Se distances. On the other hand, the small peak found at 2.4 \AA is indicative of homopolar Se—Se bonding. This accounts for 2.5% of bonds involving Se atoms, the coordination number n_{SeSe} being equal to 0.10. The sharp peak in the pair correlation functions $g_{\text{SiSe}}(r)$ stems from the largely predominant heteropolar Si-Se bonding, as expressed by the coordination number $n_{\text{SiSe}} = 3.89$. We obtain partial coordination numbers $n_{\text{Si}} = 3.95$ and $n_{\text{Se}} = 2.04$ very close to the values associated to a perfect chemically ordered tetrahedral network (CON) ($n_{\text{Si}}^{\text{CON}} = 4$, $n_{\text{Se}}^{\text{CON}} = 2$). Heteropolar bonding is known as highly favored in $\alpha\text{-SiSe}_2$ [10]. In the experiments, the fraction of homopolar bonds has been estimated close to 1%, consistently with coordination numbers only slightly deviating from the CON values [3,11]. Our results are in good agreement with this picture, as confirmed by visual inspection of Fig. 3. We found that 93% of Si atoms and 95% of Se atoms are fourfold and twofold coordinated, respectively, this percentages reducing to 87% and 85% if only chemically

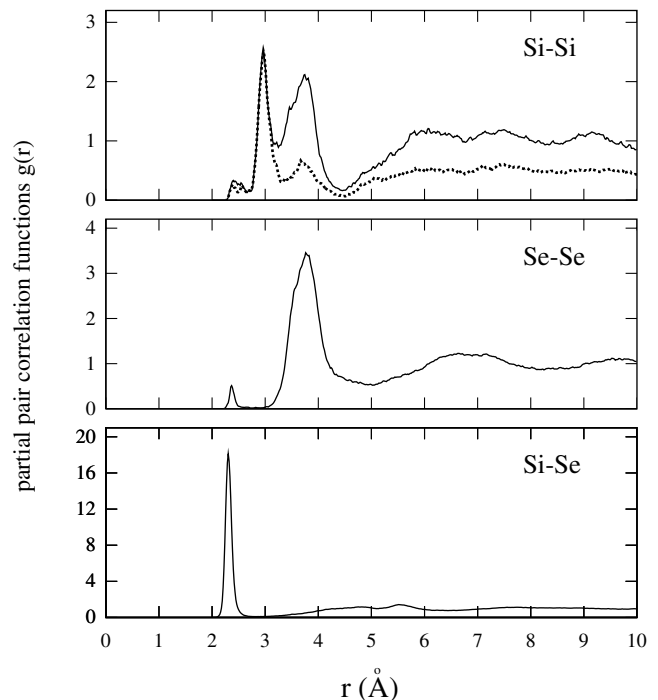


FIG. 2. Partial pair correlation functions of $\alpha\text{-SiSe}_2$. The dotted line in the uppermost panel refers to the partial pair correlation function $g_{\text{SiSi}}(r)$ calculated by considering only Si atoms in edge-sharing configurations.

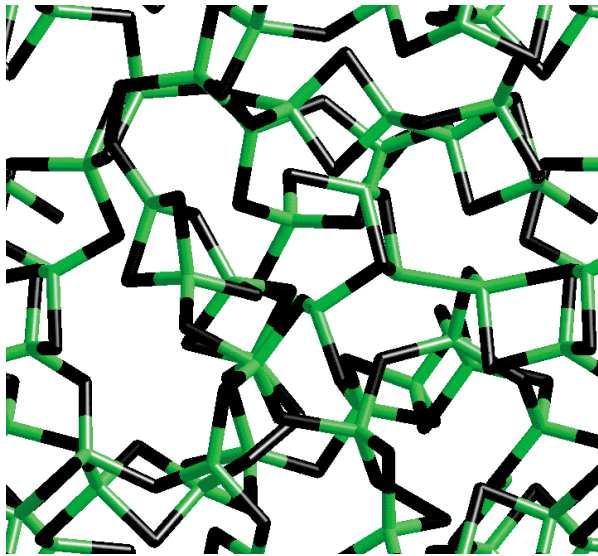


FIG. 3 (color online). A snapshot of an instantaneous configuration of amorphous SiSe_2 . Black sticks depart from Se atoms and gray sticks from Si atoms. Two atoms are connected when their mutual distance is smaller than 2.8 \AA . The system has been periodically extended in the three directions.

ordered SiSe_4 and SeSi_2 configurations are considered. A limited amount of Se (Si) atoms (3%, Se; 2%, Si) are threefold coordinated to Si (Se) atoms. Chemical order is reflected by the predominance of fourfold units and sixfold units in the ring distribution, while homopolar bonding causes the appearance of a few fivefold rings.

A key quantity to link theory with MAS-NMR data [13] on $a\text{-SiSe}_2$ is the number of Si(0), Si(1), and Si(2) sites. As shown in Table I our results are of unprecedented quality. In particular the values for Si(0) and the total number of edge-sharing Si atoms, Si(1) + Si(2) improve significantly upon the results obtained with interatomic potentials. The question arises on the role played by Si(1) and Si(2) atoms in forming chains of connected tetrahedra, often invoked in the interpretation of experiments [14]. According to classical MD studies, Si(1)-Si(2)-Si(1) is the predominant sequence of three tetrahedra with a central Si(2) atom [15]. This same structural unit emerges

TABLE I. Percentages of Si atoms which do not belong to fourfold rings [Si(0)] which belong to one fourfold ring [Si(1)] and to two fourfold rings [Si(2)]. Statistical errors in our results ($a\text{-SiSe}_2$) do not exceed 15%. We list also results from experiments ($ex\text{-}a\text{-SiSe}_2$) (Ref. [13]), and classical molecular dynamics (CMD- $a\text{-SiSe}_2$) (Ref. [15]).

	CMD- $a\text{-SiSe}_2$	$ex\text{-}a\text{-SiSe}_2$	$a\text{-SiSe}_2$
Si(0)	48	26	30
Si(1)	46	52	61
Si(2)	6	22	9

from cluster calculations in an attempt to rationalize Raman findings [16].

The distribution of Si (X)-centered sequences ($X = 0, 1, 2$) is given in Table II. First we determined the Se atoms which are common nearest neighbors of Si atoms and then we accounted for all possible paths connecting three Si atoms through shared Se atoms. Relevant sequences of ES and CS connections among tetrahedra can be traced back in the fragment of the $a\text{-SiSe}_2$ structure which is depicted in Fig. 4. As shown in Table II, the highest value for Si triads is found in the case of Si(1)-Si(0)-Si(0) and Si(1)-Si(1)-Si(0), followed by Si(1)-Si(1)-Si(1) and Si(1)-Si(0)-Si(1). These configurations arise from CS and ES connections and do not necessarily involve any miscoordination. Focusing on the Si(2)-centered triads, Si(1)-Si(2)-Si(1) is by far the most frequent, while Si(2)-Si(2)-Si(2) chains (crystallinelike) are absent. Among the 18 sequences of three neighboring Si atoms, seven are made possible by the presence of threefold Se atoms, corresponding to two adjacent fourfold rings sharing one Si-Se bond. However, the number of these configurations does not exceed 1. It appears that the count of sequences expected to characterize the network cannot be restricted to only one kind of intertetrahedral connection, i.e., the ES ones proposed on the basis of cluster calculations [16], but it has to include combinations of both ES and CS. Our results are fully compatible with recent Raman scattering findings on the stiffness transition in $\text{Si}_x\text{Se}_{1-x}$ glasses [12]. For $x > 0.27$, the network is rigid [20] and made of ES chains crosslinked by CS units or CS chains. The configuration shown in Fig. 4 follows closely the structural model proposed in Fig. 16 of Ref. [12].

By an appropriate treatment of chemical bonding via first principles molecular dynamics simulations we have obtained a description of amorphous SiSe_2 in good agreement with both neutron diffraction data and NMR experiments. Our results provide an accurate atomic-scale counterpart for network models based on bond-constraints theory [20]. Crystallinelike chains composed exclusively by ES atoms lying in two fourfold rings are absent. Some fragments of chains involving ES connections only are found in the structure. However, they are

TABLE II. Number of triads centered on the Si(0), Si(1), and Si(2) types of Si atoms. Configurations occurring via a threefold Se atom are given in bold. “2”, “1”, “0” stand for Si(2), Si(1), and Si(0), respectively. Statistical errors do not exceed 15%.

1-2-1	5	2-1-1	6	0-0-0	9
2-2-2	...	2-1-0	7	1-0-0	31
0-2-2	...	2-1-2	1	1-0-1	14
1-2-2	1	1-1-0	24	2-0-2	...
0-2-0	...	1-1-1	21	2-0-1	1
0-2-1	1	0-1-0	6	2-0-0	...

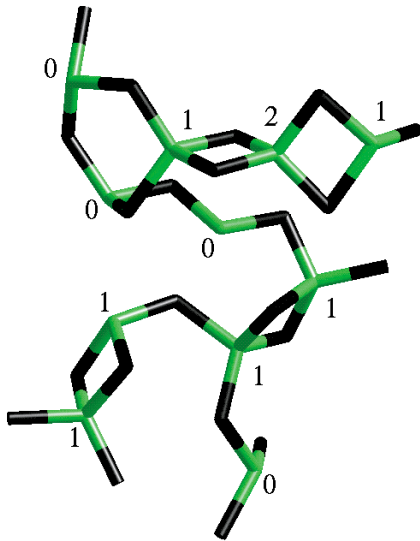


FIG. 4 (color online). A subset of configurations highlighting the kind of possible intertetrahedral connections giving rise to sequences of Si atoms (see Table II). Si atoms are labeled “0”, “1”, or “2”, according to their being part of zero [Si(0)], one [Si(1)], or two [Si(2)] fourfold rings. The following triads of Si atoms can be identified: 0—0—0, 1—0—0, 1—1—0, 1—1—1, 2—1—0, and 1—2—1.

definitely less important than those made of CS and ES tetrahedra and cannot be taken as dominant structural motif. We conclude that the structure of amorphous SiSe₂ results from the combination of cross-linked corner- and edge-sharing SiSe₄ units, both essential to achieve a complete picture of this disordered network.

Calculations have been carried out on the computers of the IDRIS center located in Orsay (France).

-
- [1] P. Boolchand and W.J. Bresser, *Nature (London)* **410**, 1070 (2001).
 [2] S. R. Elliott, *Nature (London)* **354**, 445 (1991).

- [3] P. Boolchand and W. J. Bresser, *Philos. Mag. B* **80**, 1757 (2000).
 [4] M. Tenhover, M. A. Hazle, R. K. Grasselli, and C. W. Thompson, *Phys. Rev. B* **28**, 4608 (1983).
 [5] J. E. Griffiths, M. Malyj, G. P. Espinosa, and J. P. Remeika, *Phys. Rev. B* **30**, 6978 (1984).
 [6] S. Sugai, *Phys. Rev. B* **35**, 1345 (1987).
 [7] D. L. Price, S. C. Moss, R. Reijers, M. L. Saboungi, and S. Susman, *J. Phys. C* **21**, L1069 (1988).
 [8] J. Peters and B. Krebs, *Acta Crystallogr. Sect. B* **B38**, 1270 (1982).
 [9] J. E. Griffiths, M. Malyj, G. P. Espinosa, and J. P. Remeika, *Solid State Commun.* **53**, 587 (1985).
 [10] R. W. Johnson, D. L. Price, S. Susman, M. Arai, T. I. Morrison, and G. K. Shenoy, *J. Non-Cryst. Solids* **83**, 251 (1986).
 [11] M. Arai, D. L. Price, S. Susman, K. J. Volin, and U. Walter, *Phys. Rev. B* **37**, 4240 (1988).
 [12] D. Selvanathan, W. J. Bresser, and P. Boolchand, *Phys. Rev. B* **61**, 15 061 (2000).
 [13] M. Tenhover, R. D. Boyer, R. S. Henderson, T. E. Hammond, and G. A. Shave, *Solid State Commun.* **65**, 1517 (1988).
 [14] L. F. Gladden and S. R. Elliott, *Phys. Rev. Lett.* **59**, 908 (1987).
 [15] G. A. Antonio, R. K. Kalia, A. Nakano, and P. Vashishta, *Phys. Rev. B* **45**, 7455 (1992).
 [16] K. Jackson and S. Grossman, *Phys. Rev. B* **65**, 012206 (2001).
 [17] The simulations were performed using for norm-conserving pseudopotentials the computer program described in A. Pasquarello, K. Laasonen, R. Car, C. Lee, and D. Vanderbilt, *Phys. Rev. Lett.* **69**, 1982 (1992); and in K. Laasonen, A. Pasquarello, R. Car, C. Lee, and D. Vanderbilt, *Phys. Rev. B* **47**, 10142 (1993).
 [18] J. P. Perdew, J. A. Chevary, S. H. Vosko, K. A. Jackson, M. R. Pederson, D. J. Singh, and C. Fiolhais, *Phys. Rev. B* **46**, 6671 (1992).
 [19] A. Dal Corso, A. Pasquarello, A. Baldereschi, and R. Car, *Phys. Rev. B* **53**, 1180 (1996).
 [20] M. F. Thorpe, in *Insulating and Semiconducting Glasses*, edited by P. Boolchand (World Scientific, Singapore, 2000), p. 95.